

Purdue University
Purdue e-Pubs

International Compressor Engineering Conference

School of Mechanical Engineering

1990

Gas Pulsations in Screw Compressors - Part II: Dynamics of Discharge System and It's Interaction With Port Flow

K. Koai

Purdue University

W. Soedel

Purdue University

Follow this and additional works at: <https://docs.lib.purdue.edu/icec>

Koai, K. and Soedel, W., "Gas Pulsations in Screw Compressors - Part II: Dynamics of Discharge System and It's Interaction With Port Flow" (1990). *International Compressor Engineering Conference*. Paper 727.
<https://docs.lib.purdue.edu/icec/727>

This document has been made available through Purdue e-Pubs, a service of the Purdue University Libraries. Please contact epubs@purdue.edu for additional information.

Complete proceedings may be acquired in print and on CD-ROM directly from the Ray W. Herrick Laboratories at <https://engineering.purdue.edu/Herrick/Events/orderlit.html>

GAS PULSATIONS IN TWIN SCREW COMPRESSORS -PART II: DYNAMICS OF DISCHARGE SYSTEM AND ITS INTERACTION WITH PORT FLOW

by
Kwang-lu Koai and Werner Soedel
Ray W. Herrick Laboratories
School of Mechanical Engineering
Purdue University
West Lafayette, IN 47907

Abstract

Dynamic transfer functions based on four pole arguments are formulated for a typical discharge system. Various models, such as a lumped Helmholtz model, a one dimensional wave motion model and a three dimensional finite element model are discussed. An iterating method that couples the time domain calculations of port flow to the frequency domain transfer functions is applied to predict pressure pulsations under various conditions. Typical comparisons to experimental data are shown also.

Introduction

A typical discharge system of a twin screw compressor is made up of a series of cavities and their connecting elements, which may be a muffler, a pipe section or a perforated plate. Mathematical simulation of the gas pulsation in the discharge system can be performed by first determining the pressure transfer function of the system based on its geometry and the medium's acoustic properties, and then multiplying the transfer function by the Fourier components of the discharge gas flow. Figure 1 shows the general procedure of such a process. Three different models were investigated, namely a lumped parameter model, a one dimensional continuous model and a three dimensional finite element model. The first two models utilize the four pole parameter matrices to simulate each element of the system before establishing the transfer functions of the system. The third one can access the transfer functions directly.

Four Pole Parameter Matrices and Pressure Transfer Functions

The four pole parameter matrix \widetilde{T}_m is defined as the transfer matrix which correlates the inlet and outlet conditions of an acoustic element as follows:

$$\begin{pmatrix} Q_{in} \\ P_{in} \end{pmatrix} = \widetilde{T}_m \begin{pmatrix} Q_{out} \\ P_{out} \end{pmatrix} \quad \text{where} \quad \widetilde{T}_m = \begin{bmatrix} C_{11} & C_{12} \\ C_{21} & C_{22} \end{bmatrix}$$

Q_{in} , P_{in} are the state variables (volumetric flow and dynamic pressure in this case) at the inlet of the element and Q_{out} , P_{out} are the state variables at the outlet of the element. The four pole parameters C_{11} , C_{12} , C_{21} and C_{22} for the acoustic analysis of our discharge system can be derived from linear gas dynamic theories.

The overall four pole parameter matrix of a system \widetilde{T}_{ma} is the multiplication of all the element matrices along the transfer direction (from the inlet end to the outlet end of the system).

$$\begin{pmatrix} Q_o \\ P_o \end{pmatrix} = \widetilde{T}_{ma} \begin{pmatrix} Q_{end} \\ P_{end} \end{pmatrix}$$

where $\widetilde{T}_{ma} = \widetilde{T}_{m1} \widetilde{T}_{m2} \cdots \widetilde{T}_{mn}$

The pressure transfer function P_{qx} is the dynamic pressure at location x in response to a unit harmonic volume flow of frequency ω at the inlet end and is used to

characterize an acoustic system in the frequency domain. In terms of P and Q as stated above, it is :

$$P_{qx}(\omega) \equiv \frac{P_x(\omega)}{Q_o(\omega)}$$

Procedures for calculating pressure transfer functions based on the four pole parameters obtained are:

(1) Form the overall four pole parameter matrix of the system.

$$\begin{Bmatrix} Q_o \\ P_o \end{Bmatrix} = \overline{T}_{ma} \begin{Bmatrix} Q_{end} \\ P_{end} \end{Bmatrix}$$

(2) Let Q_o be unity, select a suitable boundary condition for the end, then solve Q_{end} and P_{end} .

(3) Form a new overall four pole parameter matrix for the subsystem located in between point x and the end of the system.

$$\begin{Bmatrix} Q_x \\ P_x \end{Bmatrix} = \overline{T}_{mx} \begin{Bmatrix} Q_{end} \\ P_{end} \end{Bmatrix}$$

(4) Solve for P_x , which by definition is the transfer functions.

All the above values for P, Q, P_{qx} and C are complex numbers to account for the amplitude and phase aspects of these variables. They are all frequency dependent too.

Acoustic Models

For an exhaust system of a typical twin screw compressor as shown in Figure 2, it may be simulated in several ways: (1) If all the elements in the exhaust system are treated as volumes and necks, the lumped parameter model as shown in Figure 4 is obtained. (2) If one dimensional duct elements are chosen, the model is 1-D continuous as shown in Figure 5. (3) If combined lumped and one dimensional elements are adopted, it may look like Figure 6. (4) If the system is viewed as three dimensional and continuous, we may discretize the whole enclosure into small elements and use finite element method to solve the transfer function as shown in Figure 3. The formulation process of the 8 node isoparametric acoustic element is discussed in Appendix (A). The pressure transfer function in this case means the dynamic pressure response at the node point of interest to the unit excitation of gas flow at the source node.

Figures 7, 8, 9 and 10 show the pressure transfer functions of the exhaust system of the example screw compressor. They were derived from the above models without considering damping effect occurring at the boundaries and the absorption/attenuation of sound waves in the medium. For the finite element model, 141 elements and 322 nodes were used in discretizing the exhaust system.

A discussion about the limitations of using the lumped parameter model and the one dimensional duct model is given in Appendix (A). A simplified geometry was assumed for the discussion but the principles can be applied to any enclosure.

Interaction with the Compression Process

As has been discussed in part I of this paper, the gas flow generated at the inlet of the exhaust system during the discharge process of the compressor is periodic and can be decomposed into its Fourier series components:

$$Q_s(t) = \sum_{n=-\infty}^{\infty} Q_o(n\omega_0) e^{jn\omega_0 t}$$

where ω_0 is the fundamental frequency of the excitation flow defined as :

$$\omega_0 = 2\pi n N$$

where n is the male rotor lobe number and N is the rotation speed of the driving rotor. Because of the linear relationship between the excitation and its responses, the total

dynamic response is as follows:

$$P_i(t) = \sum_{n=-\infty, n \neq 0}^{\infty} Q_o(n \omega_o) P_q(n \omega_o) e^{j n \omega_o t}$$

Note that the zero n value is excluded from the summation because only the dynamic pressure is calculated. Steady or non-oscillatory flow does not excite gas pulsation in the discharge system.

The pressure pulsation occurring at the discharge end of the compressor may affect the flow pulsation there, and vice versa. This effect can be taken into account by adding the pulsation pressure to the steady part of the discharge pressure and iterate the thermodynamic analysis of the compressor and the acoustic analysis of the discharge system alternatively. For the example compressor, it shows that the iteration process converges very quickly (within ten cycles) and the interaction effect is negligible because the pulsation pressure is very small in comparison to the total discharge pressure.

Gas Pulsation Measurements and Comparison of Transfer Functions

A typical result of gas pulsation measurement is shown in Figure 11. The measurements which we conducted at all loads and within the reasonable operating range of the screw compressor discharge pressure show that the lowest two harmonics are most significant in their contribution to the total pulsation. We will limit ourselves to the study of lower frequency responses of gas pulsation in the screw compressor partly because of this relative significance. Also since we use the acoustic properties of the dry refrigerant gas in lieu of the true gas/oil mixture in the models, we expect that the pulsation amplitudes will be overestimated due to negligence of the absorption and attenuation capability of the mixture. The deviation will increase gradually with frequency.

One way to check the validity of the acoustic models is to compare the predicted pressure transfer functions with the semi-empirical ones, which are obtained by dividing the measured pressure pulsation data by the predicted flow pulsation at the corresponding harmonic frequencies. The semi-empirical data, which are obtained from Figure 11 based on different models, are marked on the predicted transfer functions as shown in Figures 7, 8, 9 and 10.

Generally speaking, only a three dimensional numerical model like the finite element method can predict the transfer functions of an irregularly shaped large enclosure reasonably well, because it takes care of the variations of the dynamic pressure in all three dimensions and is not limited by wave length restrictions. However if the acoustic enclosure is relatively small as compared with the acoustic wave lengths in the frequency range of interest, the lumped parameter model can be used as a substitute without sacrificing too much accuracy. Similarly if the enclosure consists of one or more slender cavities which have cross section dimensions much smaller than the acoustic wave length, the one dimensional wave motion model can be used. This explains why the finite element model gives us better predictions and why there is a similarity of the transfer functions within the frequency range of 0 to 30 Hz of these plots. The discrepancy between the predicted and measured frequency response functions for the third or higher harmonic frequencies comes perhaps from the existence of oil droplets in the exhaust gas. These suspended particles introduce additional viscous, heat conduction and evaporation losses of the sound energy in the immediate neighborhood of the particles while the sound wave propagates. A similar situation occurring in air reported that the measured sound attenuation through the fog was several hundreds times greater than that measured in dry air at 1000Hz or higher frequencies (reference no. 5). The lumped parameter model and the one dimensional duct model can also be very helpful in evaluating qualitatively the effects of (1) Muffler in the gas path, (2) Porous materials like the steel wool demister in the discharge system, and (3) Boundary condition at the termination of the enclosure.

Summary and Conclusions:

(1) Gas pulsations in the suction/discharge systems of a twin screw compressor are excited by the unsteady but periodic flow variations at the suction/ discharge ports. The flow variations are determined based on (a) the design of the compressor (b) the suction and discharge conditions of the compressor, and (c) the medium's thermophysical properties. One way to reduce the gas pulsation levels of screw compressors is to reduce its excitation flow pulsations.

(2) The pressure transfer function of an acoustic system can be determined by employing acoustic models. The three dimensional numerical model like the finite element method is the most accurate one for calculating the transfer function of an enclosure of complex geometry. However if the enclosure dimensions are small as compared to the acoustic wave length, the lumped parameter model will save much of the computation effort and work as well. Similarly if the enclosure is shaped like a duct or a series of ducts with their cross sectional dimensions much smaller than the wave length, then the one dimensional duct model can be used. The gas pulsation levels can be reduced if the geometry of the suction or discharge manifold is changed such that the pressure transfer functions become smaller. Redesigning the existing muffler or introducing a new one is one example of such an improvement.

(3) For the oil injection type screw compressors, if the dry gas properties are used to simulate the process, the models will predict the gas pulsation levels well only at low frequencies. If higher frequency responses are demanded, the properties of the real gas/ oil mixture has to be determined before the thermodynamic and acoustic analyses. Also the oil serves as a sealing medium and has to be taken into account in estimating the effective seal path areas if more precise flow pulsation levels are demanded.

(4) With an aim to reduce its gas pulsation level, it is usually not possible to redesign a screw compressor without affecting its thermodynamic performances. The thermodynamic and acoustic analyses described in this paper can evaluate the flow capacity, the power consumption rate and the gas pulsation level of the screw compressor at the same time.

References

- (1)W. Soedel, "Gas Pulsations in Compressor and Engine Manifolds" Short Course Text Book of Purdue Compressor Technology Conference, Ray W. Herrick Labs., School of Mechanical Engineering, Purdue University, 1978.
- (2)J. Kim, W. Soedel, "Simulation of a High Speed Hermetic Compressor with Special Attention to Gas Pulsations in Three Dimensional Continuous Cavities" Ph.D.Thesis, Ray W. Herrick Labs., School of Mechanical Engineering, Purdue University, Feb. 1988.
- (3)C.H.Kung, "Finite Element and Experimental Modeling of Three-dimensional Annular-like Acoustic Cavities using the Normal Mode Approach" Ph.D.Thesis, The Ohio State University, 1984.
- (4)R.Bernhard, S.Takeo "A finite Element Procedure for Design of Cavity Acoustical Treatments" J.Acoust.Soc.Am.83(6), June 1988.
- (5)V.O.Knudsen,J.V.Wilson and N.S.Anderson "The Attenuation of Audible Sound in Fog and Smoke" J.Acoust.Soc.Am.20(6), Nov 1948

Acknowledgement

The support of this work by United Technologies Carrier is gratefully acknowledged.

Appendix (A) Finite Element Formulation for Finding the Pressure Transfer Functions of an Enclosure

Differential equation for the dynamic pressure $p = p(x, y, z, t)$:

$$\frac{1}{C^2} \frac{\partial^2 p}{\partial t^2} = \frac{\partial^2 p}{\partial x^2} + \frac{\partial^2 p}{\partial y^2} + \frac{\partial^2 p}{\partial z^2} + q(t) \delta(x-x_0) \delta(y-y_0) \delta(z-z_0)$$

where q is the first time derivative of the mass generation rate occurring at point (x_0, y_0, z_0)

The pressure transfer function $P_{qx}(\omega)$ is the dynamic pressure at an arbitrary point (x, y, z) in response to a unit harmonic volume flow excitation of angular velocity ω or frequency f ($\omega = 2\pi f$) at another point (x_0, y_0, z_0) . Hence

$$q(t) = \frac{d}{dt} (\rho Q_0 e^{j\omega t}) = j \omega \rho Q_0 e^{j\omega t} \text{ where } Q_0 = 1.0$$

$$p(x, y, z, t) = P(x, y, z) e^{j\omega t} = P_{qx}(\omega) e^{j\omega t}$$

Substitute into the differential equation and obtain

$$\frac{\omega^2}{C^2} P + \nabla^2 P = -j \omega \rho \delta(x-x_0) \delta(y-y_0) \delta(z-z_0)$$

The pressure and the coordinates of any point in the element can be expressed in terms of nodal pressures and coordinates based on Galerkin's formulation for an three dimensional 8 node isoparametric element with N_i as the shape functions:

$$P = \sum_{i=1}^8 P_i N_i$$

$$\text{and } x = \sum_{i=1}^8 x_i N_i, \quad y = \sum_{i=1}^8 y_i N_i, \quad z = \sum_{i=1}^8 z_i N_i$$

The mass, damping and stiffness matrices of the element can be formulated too:

$$[M] = [m_{ij}] \quad \text{where } m_{ij} = \frac{1}{C^2} \int_D N_i N_j dD$$

$$[C] = [c_{ij}] \quad \text{where } c_{ij} = \int_B \frac{\rho_0}{Z_n} N_i N_j dB$$

$$[K] = [k_{ij}] \quad \text{where } k_{ij} = \int_D \nabla N_i \nabla N_j dD$$

For rigid boundary conditions ($Z_n = \infty$), we have $c_{ij} = 0$. The global mass and stiffness matrices can be formed following a typical assemblage procedure. The global force vector can be formulated directly by putting the $-j\omega\rho$ value at the corresponding location for the excitation node point and zero at all other node points. By solving the simultaneous equations, the dynamic pressures at every point in the enclosure can be obtained.

Appendix (B) Equations and Limitations of Acoustic Models

(1) Governing equations

a. Lumped Parameter model:

$$\rho C^2 = - \frac{dP}{\left(\frac{dV}{V}\right)}$$

$$\text{or } \frac{dP}{dt} = - \frac{\rho C^2}{V} \left(\frac{dV}{dt}\right)$$

$$\text{or } P = - \left(\frac{\rho C^2}{j \omega V}\right) Q$$

b. one dimensional duct model:

$$\frac{1}{C^2} \frac{\partial^2 p}{\partial t^2} = \frac{\partial^2 p}{\partial x^2} \quad \text{and} \quad Q_0 = v_0 S$$

c. three dimension wave model:

$$\frac{1}{C^2} \frac{\partial^2 p}{\partial t^2} = \frac{\partial^2 p}{\partial x^2} + \frac{\partial^2 p}{\partial y^2} + \frac{\partial^2 p}{\partial z^2} + q(t) \delta(x-x_0) \delta(y-y_0) \delta(z-z_0)$$

(2) Application to a cubic cavity of 6.6 cm on each side

R22 gas condition: 241 psia and 180 °F, the corresponding acoustic properties are: density $52.6 \times 10^{-3} \text{ g/cm}^3$, sound speed 17740 cm/s. The predicted pressure transfer functions from different models are shown in Figure 12. The first theoretical antinode peak of this cavity occurs at 1344 Hz while the corresponding wave length is twice the side length. The three dimensional finite element model takes care of pressure variations in all three directions and is used as the comparison basis. The lumped parameter model will predict the pressure transfer functions well at a frequency lower than 800 Hz (wave length to be four times of the side length or larger) And the one dimensional duct model is good for frequency lower than 300 Hz only (wave length to be nine times of the side length or larger).

(3) A rectangular cavity of dimensions 16 cm x 2 cm x 2 cm

With the gas condition same as above (2), a comparison of the models are shown in Figure 13. The first antinode peak occurs at about 554 Hz. The one dimensional model predicts the pressure transfer functions very well if the wave length of the acoustic wave is at least eight times higher than the side length of the cross section area (higher than 1100Hz in this case). The lumped parameter model predicts the result well only at a frequency lower than 140 Hz (wave length to be eight times of the duct length or larger).

Appendix (C) Nomenclatures

∇ :	gradient operator
a:	(subscript) property of the overall system
o:	(subscript) source of the acoustic excitation
x:	(subscript) location of the pressure point of interest
ρ :	density of the medium
ω :	angular velocity
f:	frequency
j:	unit complex variable
n:	lobe number of the driving rotor
p:	acoustic or dynamic pressure (=total pressure- static pressure)
q:	first derivative of the mass flow rate
v:	acoustic particle velocity
B:	domain of surface or boundary integration
C:	speed of sound of the medium
D:	domain of space integration
N:	rotation speed of the driving rotor in rounds per second
P:	amplitude of the dynamic pressure
P_q :	pressure transfer function
Q:	volumetric flow
S:	cross section area of the pipe or duct
Z_n :	acoustic impedance at the boundary surface of the enclosure

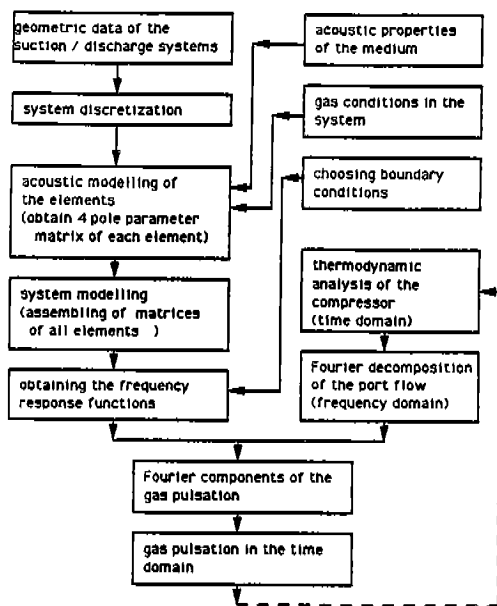


Figure 1: Procedures of Gas Pulsation Analysis

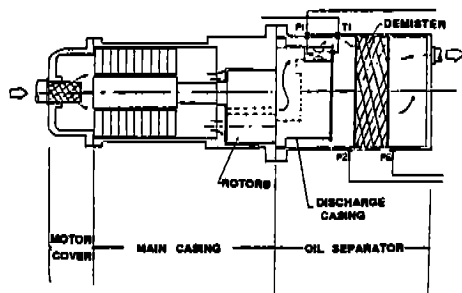


Figure 2: Suction and Discharge Systems of a Twin Screw Compressor

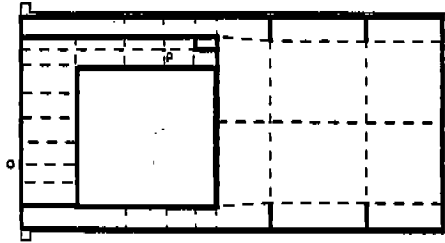


Figure 3: A Finite Element Model for the Discharge System (schematic drawing)

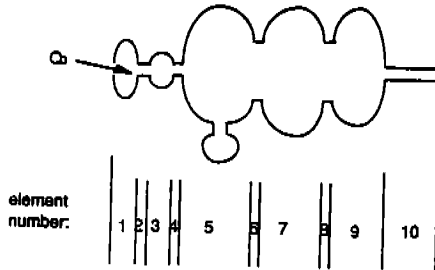


Figure 4: A Lumped Parameter Model for the Discharge System

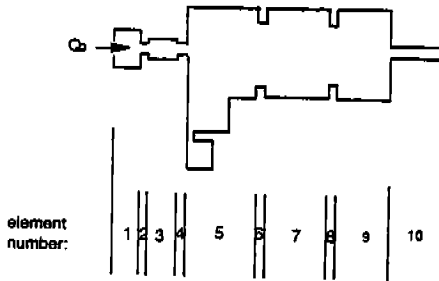


Figure 5: A Continuous Model for the Discharge System

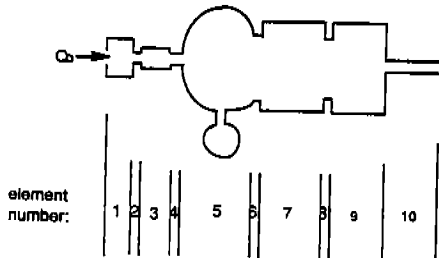


Figure 6: A Combined Model for the Discharge System

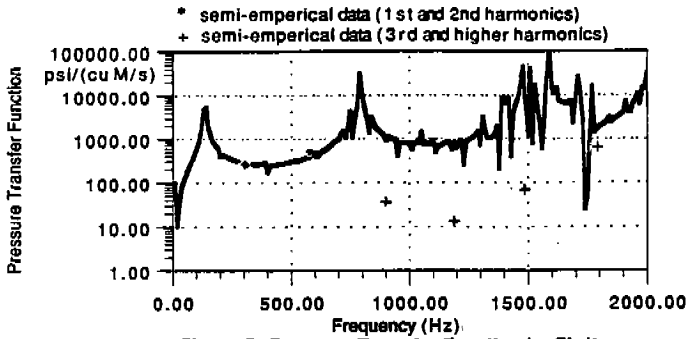


Figure 7: Pressure Transfer Function by Finite Element Model

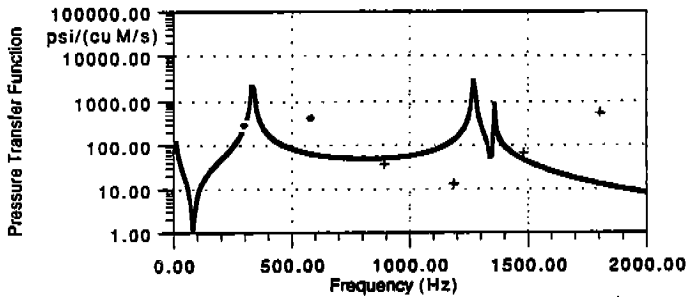


Figure 8: Pressure Transfer Function by Lumped Parameter Model

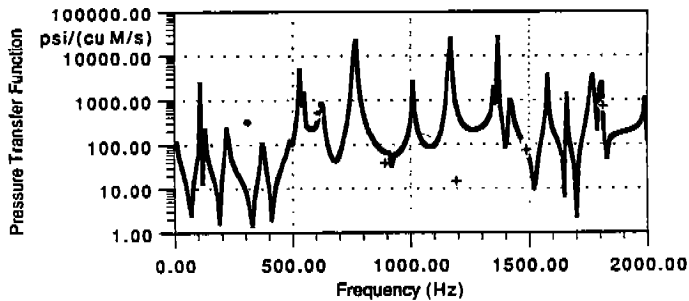


Figure 9: Pressure Transfer Function by One Dimensional Duct Model

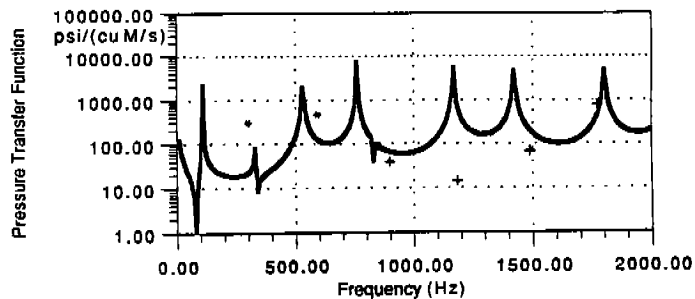


Figure 10: Pressure Transfer Function by Combined Lumped and One Dimensional Model

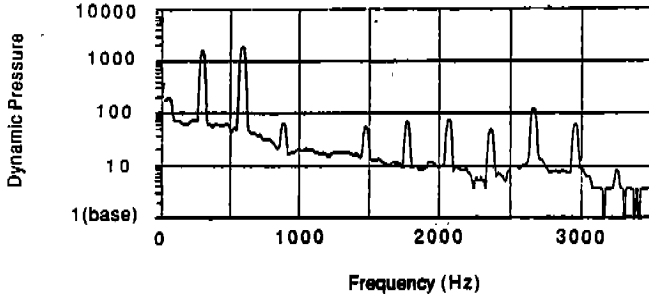


Figure 11 : Measured Gas Pulsation Levels (relative amplitudes)

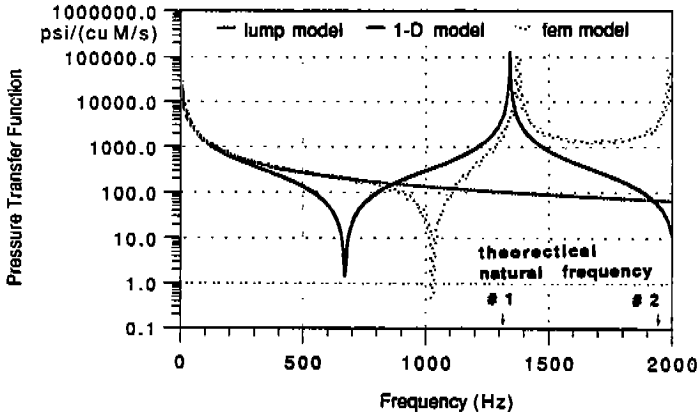


Figure 12: Pressure Transfer Functions of a Cubic Cavity with 6.6cm on Each Side

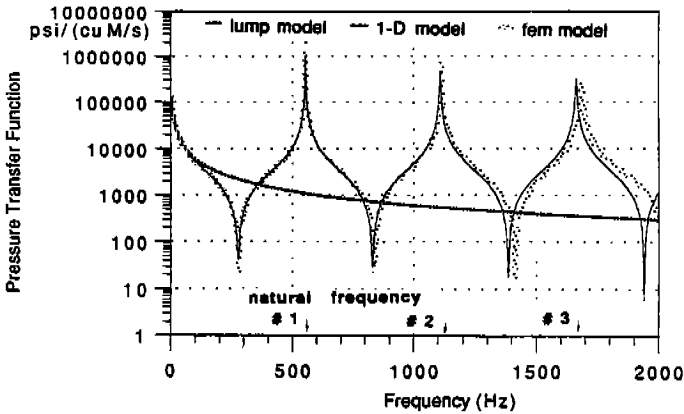


Figure 13: Pressure Transfer Functions of a Duct of Dimensions 16cmX2cmX2cm